

Optimal Control for Suppression of Singularity in Chemotaxis via Flow Advection

Weiwei Hu¹ · Ming-Jun Lai¹ · Jinsil Lee¹

Accepted: 29 February 2024
© The Author(s), under exclusive licence to Springer Science+Business Media, LLC, part of Springer Nature 2024

Abstract

This work focuses on the optimal control design for suppressing the singularity formation in chemotaxis governed by the parabolic-elliptic Patlak–Keller–Segel (PKS) system via flow advection. The main idea of this work lies in utilizing flow advection for enhancing diffusion as to control the nonlinear behavior of the system. The objective is to determine an optimal strategy for adjusting flow strength so that the possible finite time blow-up of the solution can be suppressed. Rigorous proof of the existence of an optimal solution and derivation of first-order optimality conditions for solving such a solution are presented. Spline collocation methods are employed for solving the optimality conditions. Numerical experiments based on 2D cellular flows in a rectangular domain are conducted to demonstrate our ideas and designs.

Keywords Optimal control · Flow advection · Chemotaxis · Patlak–Keller–Segel system · Suppression of singularity · Cellular flows · Spline collocation methods

1 Introduction

This work discusses the problem of optimal control design for suppression of singularity formation in chemotaxis via flow advection. Chemotaxis is the movement of cells in response to a chemical stimulus. A coupled parabolic system was first employed to model this process by Patlak [33], Keller and Segel in [21, 22], which describes the evolving densities of one or more chemotactic population and its attractants/repellents. Other related study and reviews can be found in (e.g. [15, 16, 34, 39, 40]). The current

☑ Weiwei Hu Weiwei.Hu@uga.edu

Ming-Jun Lai mjlai@uga.edu

Jinsil Lee jinsil.lee@uga.edu

Published online: 12 April 2024



Department of Mathematics, University of Georgia, Athens, GA 30602, USA

work focuses on a simplified parabolic-elliptic Patlak–Keller–Segel (PKS) equations introduced by Nagai in [32] (also see [19]) with flow advection or a drift, induced by the movement of the ambient fluid, in an open bounded and connected domain $\Omega \subset \mathbb{R}^d$, d = 2, 3, with a smooth boundary Γ (corners may be allowed).

Let $\theta \ge 0$ be the density of the cells and $c \ge 0$ be the concentration of a chemoattractant produced by the cells. Further, let $\mathbf{v} = \mathbf{v}(x)$ be a predetermined time-independent incompressible flow and u = u(t) be a time-dependent control input regulating the strength of the flow. The system with controlled flow advection is governed by

$$\frac{\partial \theta}{\partial t} = \Delta \theta - u(t)\mathbf{v} \cdot \nabla \theta - \nabla \cdot (\theta \chi \nabla c) \quad \text{in} \quad \Omega, \tag{1.1}$$

$$-\Delta c + c = \theta \quad \text{in} \quad \Omega, \tag{1.2}$$

$$\nabla \cdot \mathbf{v} = 0 \quad \text{in} \quad \Omega, \tag{1.3}$$

with Neumann boundary conditions for both $\theta \geq 0$ and $c \geq 0$, no-penetration condition for ${\bf v}$

$$\frac{\partial \theta}{\partial \mathbf{n}} = \frac{\partial c}{\partial \mathbf{n}} = 0 \quad \text{and} \quad \mathbf{v} \cdot \mathbf{n} = 0 \quad \text{on} \quad \Gamma, \tag{1.4}$$

and the initial condition

$$\theta(x,0) = \theta_0(x) \text{ in } \Omega,$$
 (1.5)

where $\chi > 0$ is a sensitivity parameter of the cells to the chemo-attractant c and \mathbf{n} is the outward unit normal vector to the domain boundary Γ . The objective is to seek for an optimal regulating function u(t) for the ambient fluid as to suppress the possible finite time blow-up. It is well-studied that in the absence of flow advection or the drift, if the initial condition is above certain critical threshold, the solution of the PKS equations may blow up in finite time by concentrating positive mass at a single point (e.g. [11–14, 19]). With flow advection, however, for any initial distribution there exists an ambient velocity field \mathbf{v} , either time-independent or dependent, such that the solution to (1.1)–(1.5) is globally regular for all positive time [23]. Singularity formation can be prevented via flow advection by mixing the cell in the direction that mitigates concentration.

When u(t) = A > 0 is a constant, Iyer, Xu and Zlatoš in [18] showed that if the flow has small dissipation times [18, Definition 1.1], then the global well-posedness result can be obtained in torus \mathbb{T}^d , d = 2, 3. The case with A < 0 can be treated similarly by letting \mathbf{v} be $-\mathbf{v}$. In fact, the small dissipation times can be achieved by increasing A, if

the operator $\mathbf{v} \cdot \nabla$ has no eigenfunctions in $H^1(\Omega)$ other than the constant function. (1.6)



This condition was established in [4] to characterize what flows enhance diffusion. The incompressible flow **v** satisfying (1.6) is so-called *relaxation enhancing* [4, Definition 1.1]. However, it is rather complex to construct such flows and many flows in real-world applications do not necessarily possess this property. The authors in [18] further showed that the flows with arbitrarily small dissipation times can be constructed by rescaling a general class of smooth (time-independent) cellular flows, which does not necessarily satisfy (1.6). The proof is based on the probabilistic method. Similar results were obtained by using a semigroup approach by Hu in [17] for the PKS system in a general bounded domain. The detailed discussion is presented in Sect. 2. Other related work on suppression of singularity by shear flows can be also found in (e.g. [2]).

In the rest of our discussion, we set $\chi = 1$. If θ is the solution to the PKS system (1.1)–(1.5), with boundary conditions in (1.4) it is easy to verify that the spatial average

$$\bar{\theta}(t) = \frac{1}{|\Omega|} \int_{\Omega} \theta \, dx = \frac{1}{|\Omega|} \int_{\Omega} \theta_0 \, dx = \bar{\theta}_0, \quad \forall t > 0.$$
 (1.7)

In fact, by Stokes formula we have

$$\begin{split} \frac{\partial \int_{\Omega} \theta \, dx}{\partial t} &= \int_{\Omega} \Delta \theta \, dx - u \int_{\Omega} \mathbf{v} \cdot \nabla \theta \, dx - \int_{\Omega} \nabla \cdot (\theta \, \chi \, \nabla c)) \, dx \\ &= \int_{\Gamma} \frac{\partial \theta}{\partial \mathbf{n}} \, dx - u (\int_{\Gamma} \mathbf{v} \cdot \mathbf{n} \theta \, dx - \int_{\Omega} \nabla \cdot \mathbf{v} \theta \, dx) - \int_{\Gamma} (\theta \, \chi \, \nabla c) \cdot \mathbf{n} \, dx = 0, \end{split}$$

thus (1.7) follows. It is shown in [17, Theorem 2.2] that for $\theta_0 \in L^2(\Omega)$ if (1.6) holds, then there exists a constant $u(t) = A = A(\theta_0) > 0$ depending on θ_0 , such that the solution to (1.1)–(1.5) is globally regular for all t > 0 and θ converges to its spatial average $\bar{\theta}$ exponentially. These results lay a theoretical foundation for our optimal control design for suppression of singularity formation.

1.1 Control Design via Flow Advection

Although there is rich literature on optimal control for chemotaxis, it predominantly focuses on the linear distributed control of the chemoattractant (e.g. [35–37]) or bilinear control of the cells or chemoattractant of the form $u\theta$ or uc (e.g. [6, 8, 9]), where u = u(x, t) is the control input. This is the first work, to our best knowledge, to control the PKS system via active control of the flow advection. We aim at designing an optimal input u(t) for regulating the flow so that the possible blow-up in solution can be suppressed and the solution is as close as possible to its its spatial average. In this work, we assume that u(t) has both upper and lower bounds. Let the set of admissible control be

$$U_{ad} = \{ u \in L^2(0, t_f) : \underline{u} \le u \le \overline{u} \},$$

where $\underline{u} < 0 < \overline{u}$ and \overline{u} is allowed to depend on the initial datum θ_0 . We seek $u \in U_{ad}$ that minimizes the following cost functional



$$J(u) = \frac{\alpha}{2} \|\theta(t_f) - \bar{\theta}\|_{L^2}^2 + \frac{\beta}{2} \int_0^{t_f} \|\theta(t) - \bar{\theta}\|_{L^2}^2 dt + \frac{\gamma}{2} \int_0^{t_f} |u|^2 dt, \tag{1.8}$$

for a given final time $t_f>0$, subject to (1.1)–(1.5), where $\alpha,\beta\geq 0$ and $\gamma>0$ are the state and control weight parameters, respectively. The parameters α and β do not vanish simultaneously. We first show that the optimal problem (1.8) is well-posed, that is, for any given initial datum $\theta_0\in L^2(\Omega)$, there exits a control $u\in U_{ad}$ such that $J(u)<\infty$. To this end, it is critical to understand the well-posedness of the PKS system in the presence of flow advection in bounded domains and choose appropriate bounds for u(t) so that U_{ad} is non-empty. Then we proceed to prove the existence of an optimal solution to problem (P). Since we have a nonlinear system associated with a nonlinear control input, problem (P) is no longer convex. As a result, the optimal solution may not be unique.

To start with, we let $\vartheta = \theta - \bar{\theta}$, then $\bar{\vartheta}(t) = 0$ for $t \ge 0$, and ϑ satisfies

$$\frac{\partial \vartheta}{\partial t} = \Delta \vartheta - u(t)\mathbf{v} \cdot \nabla \vartheta - \nabla \cdot ((\vartheta + \bar{\theta})\nabla c) \quad \text{in} \quad \Omega, \tag{1.9}$$

$$-\Delta c + c = \vartheta + \bar{\theta} \quad \text{in} \quad \Omega, \tag{1.10}$$

$$\nabla \cdot \mathbf{v} = 0 \quad \text{in} \quad \Omega, \tag{1.11}$$

$$\frac{\partial \vartheta}{\partial \mathbf{n}} = \frac{\partial c}{\partial \mathbf{n}} = 0 \quad \text{and} \quad \mathbf{v} \cdot \mathbf{n} = 0 \quad \text{on} \quad \Gamma, \tag{1.12}$$

$$\vartheta(x,0) = \theta_0(x) - \bar{\theta} \quad \text{in} \quad \Omega. \tag{1.13}$$

The cost functional in (1.8) can be rewritten as

$$J(u) = \frac{\alpha}{2} \|\vartheta(t_f)\|_{L^2}^2 + \frac{\beta}{2} \int_0^{t_f} \|\vartheta(t)\|_{L^2}^2 dt + \frac{\gamma}{2} \int_0^{t_f} |u|^2 dt, \tag{P}$$

subject to the translated system (1.9)–(1.13).

The rest of this work is organized as follows. In Sect. 2, we first present the global well-posedness and regularity properties of the PKS system in a bounded domain, which pave a way for establishing the well-posedess of the optimal control problem (*P*) and the existence of an optimal solution. In Sect. 3, we derive the first-order optimality conditions for solving the optimal solution using the variational inequality (e.g. [31]). Finally, in Sect. 4 we use the spline collocation method for implementing the optimality system (e.g. [1, 10, 24, 25]). Numerical experiments based on 2D cellular flows for suppression of singularity in rectangle domains will be presented to demonstrate the effectiveness of our control design.

2 Well-Posedness of the PKS System and Existence of an Optimal Control

We first consider u(t) = A being a parameter which regulates the strength of the flow. The flow velocity \mathbf{v} is always assumed to be time-independent and divergence free



with $\mathbf{v} \cdot \mathbf{n}|_{\Gamma} = 0$. It is proven in [17] that the global well-posedness of the PKS system can be obtained in an appropriate Hilbert space H if the analytic semigroup generated by the advection–diffusion operator $\Delta - A\mathbf{v} \cdot \nabla$, denoted by $S_A(t)$, $t \ge 0$, has a *rapid decay property* on H. That is, there exist $M_0 \le 1$ and $\omega_A > 0$ such that

$$||S_A(t)||_{\mathcal{L}(H)} \le M_0 e^{-\omega_A t}, \quad t \ge 0,$$
 (2.1)

where ω_A can be made arbitrarily large by adjusting A and M_0 is independent of ω_A . Here $\mathcal{L}(H)$ stands for the set of bounded linear operators on H and $\|\cdot\|_{\mathcal{L}(H)}$ stands for the operator norm.

Let $H = L_0^2(\Omega) = \{ \psi \in L^2(\Omega) : \int_{\Omega} \psi \, dx = 0 \}$ be the subspace of mean zero functions. Define

$$\mathcal{L}_{A} = \Delta - A\mathbf{v} \cdot \nabla$$

with $D(\mathcal{L}_A) = \{ \phi \in H^2(\Omega) \cap H : \frac{\partial \phi}{\partial \mathbf{n}} |_{\Gamma} = 0 \}$. Then $-\mathcal{L}_A$ is *m*-accretive (e.g. [20, p. 279]). A closed operator $-\mathcal{L}_A$ in a Hilbert space H is called *m*-accretive if the left open half-plane is contained in its resolvent set $\varrho(-\mathcal{L}_A)$ with

$$(-\mathcal{L}_A + \lambda)^{-1} \in \mathcal{L}(H), \quad \|(-\mathcal{L}_A + \lambda)^{-1}\| \le \Re \lambda^{-1} \quad \text{for } \Re \lambda > 0.$$

Define

$$\Psi(\mathcal{L}_A) = \inf\{\|(\mathcal{L}_A + i\lambda)\phi\|_{L^2} \colon \phi \in D(\mathcal{L}_A), \lambda \in \mathbb{R}, \|\phi\|_{L^2} = 1\}$$
 (2.2)

as in [41]. The following Gearhart-Prüss type theorem is proven in [41, Theorem 1.3] for an *m*-accretive operator, that is,

$$\|e^{\mathcal{L}_A t}\|_{\mathcal{L}(L^2(\Omega))} \le M_0 e^{-\Psi(\mathcal{L}_A)t}, \quad t \ge 0, \tag{2.3}$$

where $M_0 = e^{\pi/2}$. Furthermore,

$$\Psi(\mathcal{L}_A) \to +\infty$$
, as $A \to +\infty$, (2.4)

if and only if

$$\mathbf{v} \cdot \nabla$$
 has no eigenfunctions in $H^1(\Omega) \cap H$. (2.5)

The relations (2.3)–(2.5) indicate that the rapid decay property (2.1) holds if (2.5) is satisfied. Further define the nonlinear operator $\mathcal{N}: H^1(\Omega) \to H$ by

$$\mathcal{N}\vartheta = -\nabla \cdot ((\vartheta + \bar{\theta})\nabla c), \tag{2.6}$$

where c can be replaced in terms of ϑ . Define the operator

$$A = -\Delta + I \tag{2.7}$$

with domain $D(A) = \{ \phi \in H^2(\Omega) : \frac{\partial \phi}{\partial \mathbf{n}} |_{\Gamma} = 0 \}$. Then A is strictly positive and self-adjoint. According to (1.10) and (1.12), we have

$$c = \mathcal{A}^{-1}(\vartheta + \bar{\theta}) = \mathcal{A}^{-1}\vartheta + \bar{\theta}.$$

Replacing u(t) by A, we can rewrite the PKS system (1.9)–(1.13) as an abstract Cauchy problem in the state space H

$$\dot{\vartheta} = \mathcal{L}_A \vartheta + \mathcal{N} \vartheta, \tag{2.8}$$

$$\vartheta(0) = \vartheta_0 \in H,\tag{2.9}$$

where the system operator \mathcal{L}_A generates an analytic semigroup, denoted by $e^{\mathcal{L}_A t}$, $t \geq$ 0, on H and the nonlinearity of operator \mathcal{N} can be characterized by the following results [17, Lemma 2.4].

Lemma 2.1 For $\vartheta \in H^1(\Omega)$, then there is a constant $C_1 > 0$ such that

$$||\mathcal{N}\vartheta||_{L^{2}} \le C_{1}(||\vartheta||_{H^{1}}^{2} + |\bar{\theta}|||\vartheta||_{L^{2}}). \tag{2.10}$$

Moreover, for $\vartheta \in L^2(\Omega)$, there is a constant $C_2 > 0$ such that

$$\|(-\mathcal{L}_A)^{-\frac{3}{4}}(\mathcal{N}\vartheta)\|_{L^2} \le C_2(\|\vartheta\|_{L^2}^2 + |\bar{\theta}|\|\vartheta\|_{L^2}). \tag{2.11}$$

The estimate (2.10) has been established in the proof of [18, Lemma 3.1] on \mathbb{T}^d , d=2,3. The following theorem on the global well-posedness and stability of the nonlinear system (2.8)–(2.9) is established in [17, Theorem 2.2], utilizing the classic tools of analytic semigroup theory for semilinear equations together with a fixed-point theorem. For simplicity, we denote $\Psi(\mathcal{L}_A)$ by Ψ_A .

Theorem 2.2 Let $\vartheta_0 \in H$ and $\mathbf{v} \in L^{\infty}(\Omega)$. If $\Psi_A = \Psi_A(\vartheta_0, \bar{\theta}) > 0$ is sufficiently large, then there exists a unique mild (weak) solution ϑ to (2.8)–(2.9) satisfying

$$\vartheta \in C([0,\infty);H) \cap L^2_{loc}(0,\infty;H^1(\Omega)) \tag{2.12}$$

and

$$\sup_{t \ge 0} \|\vartheta\|_{L^2} \le 2\|\vartheta_0\|_{L^2} + 1. \tag{2.13}$$

Moreover, there exist constants $M_* \ge 1$ and $\omega_0 > 0$ such that

$$\|\vartheta\|_{L^2} \le M_* e^{-\omega_0 t} \|\vartheta_0\|_{L^2}. \tag{2.14}$$

Using the variation of parameters formula we can express the mild solution to (2.8)–(2.9) as

$$\vartheta(t) = e^{\mathcal{L}_A t} \vartheta_0 + \int_0^t e^{\mathcal{L}_A (t - \tau)} (\mathcal{N} \vartheta)(\tau) d\tau. \tag{2.15}$$



Furthermore, by (2.10)–(2.13) we have $\Delta\theta \in L^2(0,t_f;(H^1(\Omega))')$, $\mathbf{v}\cdot\nabla\vartheta\in L^2(0,t_f;L^2(\Omega))$, and

$$\mathcal{N}\vartheta\in L^1(0,t_f;L^2(\Omega))\cap L^2(0,t_f;(D(-\mathcal{L}_A)^{3/4})'),$$

for any $0 < t_f < \infty$. Therefore, we can derive that

$$\frac{\partial \vartheta}{\partial t} \in L^2(0, t_f; (D(-\mathcal{L}_A)^{3/4})'). \tag{2.16}$$

2.1 Existence of an Optimal Control

With Theorem 2.2 at our disposal, we are in a position to show the existence of an optimal control to problem (P) subject to (1.9)–(1.13). Note that it is key to choose an appropriate $\overline{u} > 0$ such that U_{ad} is non-empty. In light of Theorem 2.2, if velocity field \mathbf{v} satisfies (2.5), then we can always make $\Psi_A = \Psi_A(\vartheta_0, \overline{\theta}) > 0$ sufficiently large by increasing A. In this case, we can simply choose $\overline{u} \geq A$ and $u(t) = \overline{u}$, then the cost functional $J(u) < \infty$ due to (2.12). In other words, U_{ad} is non-empty. However, if the velocity field is generated by cellular flows, (2.5) may not hold. Then we can set $\mathbf{v}_A = A\mathbf{v}(Ax)$ and adjust A to rescale both the cell size and the flow amplitude to make Ψ_A arbitrarily large (see Sect. 3.1).

To proceed with the existence of an optimal control, we first introduce an alternative definition of a weak solution to (2.8)–(2.9) as follows.

Definition 2.3 Let $\vartheta_0 \in L^{\infty}(\Omega)$, $u \in U_{ad}$, and $\mathbf{v} \in L^{\infty}(\Omega)$. ϑ is said to be a weak solution of system (1.9)–(1.13), if θ satisfies

$$\left(\frac{\partial \vartheta}{\partial t}, \phi\right) + (\nabla \vartheta, \nabla \phi) - u(\vartheta, \nabla \phi) - ((\vartheta + \partial)\nabla \mathbf{c}, \nabla \phi) = \mathbf{0}, \quad \forall \phi \in \mathbf{H}^{1}(\Omega),$$
(2.17)

in the distribution sense on $(0, t_f)$.

Theorem 2.4 Let $\vartheta_0 \in H$. Assume that $\mathbf{v} \in L^{\infty}(\Omega)$ is chosen such that $\Psi_A = \Psi_A(\vartheta_0, \bar{\theta}) > 0$ can be made sufficiently large via adjusting A. If the upper bound \bar{u} of the control input satisfies $\bar{u} \geq A$, then there exists an optimal solution $u(t) \in U_{ad}$ to problem (P).

Proof We start with an *a priori* estimate for choosing \overline{u} . First set u(t) = A > 0. According to Theorem 2.2, for $\vartheta_0 \in L^\infty(\Omega)$, if $\mathbf{v} \in L^\infty(\Omega)$ is chosen such that $\Psi_A = \Psi_A(\vartheta_0, \overline{\theta}) > 0$ can be made sufficiently large via adjusting A, then there exists a unique weak solution satisfying (2.17). Next we let $\overline{u} \geq A$ and employ the direct method to show the existence of an optimal control in U_{ad} . Here we simply set $\underline{u} = -\overline{u}$.

Since $J \geq 0$ is bounded from below, we may choose a minimizing sequence $\{u_m\} \subset U_{ad}$ such that

$$\lim_{m\to\infty}J(u_m)=\inf_{u\in U_{ad}}J(u)<\infty.$$

By the definition of J, the sequence $\{u_m\}$ is uniformly bounded in U_{ad} , and hence there exists a weakly convergent subsequence, still denoted by $\{u_m\}$, such that

$$u_m \to u^*$$
 weakly in $L^2(0, t_f)$.

In the worst case scenario, $u_m = u^* = \overline{u}$. Correspondingly, based on Theorem 2.2, for $\vartheta_0 \in L^{\infty}(\Omega)$ there exists a sequence of solutions $\{\vartheta_m\}$ satisfying (2.17) and $\vartheta_m \in C([0,t_f];L^2(\Omega)) \cap L^2(0,t_f;H^1(\Omega))$. Together with (2.16) we may extract a subsequence, still denoted by $\{\theta_m\}$, such that

$$\vartheta_m \to \vartheta^*$$
 weakly in $L^2(0, t_f; H^1(\Omega))$ (2.18)

$$\frac{\partial \vartheta_m}{\partial t} \to \frac{\partial \vartheta^*}{\partial t}$$
 weakly in $L^2(0, t_f; (D(-\mathcal{L}_A)^{3/4})')$. (2.19)

By Aubin–Lions lemma, (2.18)–(2.19) indicate that

$$\vartheta_m \to \vartheta^*$$
 strongly in $L^2(0, t_f; L^2(\Omega))$. (2.20)

It remains to show that ϑ^* is the solution corresponding to u^* based on Definition 2.3. Note that u_m and ϑ_m satisfy

$$(\frac{\partial \vartheta_m}{\partial t}, \phi) + (\nabla \vartheta_m, \nabla \phi) - u_m(\vartheta_m, \nabla \phi) - ((\vartheta_m + \partial) \nabla c_m, \nabla \phi) = 0, \quad \forall \phi \in \mathbf{H}^1(\Omega).$$
(2.21)

Let ψ be a continuously differentiable function on $[0, t_f]$ with $\psi(t_f) = 0$. For each $\phi \in H^1(\Omega)$, we multiply (2.21) by ψ and integrate by parts. After integrating the first term by parts, we get

$$-\int_{0}^{t_{f}} (\vartheta_{m}, \phi \dot{\psi}) dt + \int_{0}^{t_{f}} (\nabla \vartheta_{m}, \nabla \phi) \psi dt - \int_{0}^{t_{f}} u_{m}(\mathbf{v}\theta_{m}, \nabla \phi) \psi dt - \int_{0}^{t_{f}} (\vartheta_{m} \nabla c_{m}, \nabla \phi) \psi dt - \int_{0}^{t_{f}} (\bar{\theta} \nabla c_{m}, \nabla \phi) \psi dt = (\vartheta_{0}, \phi \psi(0)).$$
 (2.22)

Since $\phi \dot{\psi} \in L^2(0,T;L^2(\Omega))$ and $\nabla \phi \in L^2(\Omega)$, it is straightforward to pass to the limit in the first two terms and the last term of the left hand side of (2.22) with the help of (2.18). To estimate the second term, using the convergence results (2.18)–(2.20) we have

$$\begin{split} &\left| \int_{0}^{T} \left(\int_{\Omega} u_{m} \vartheta_{\mathbf{m}} \cdot \nabla \phi \, \mathbf{d} \mathbf{x} \mathbf{d} \mathbf{t} - \int_{\mathbf{0}}^{T} \int_{\Omega} \mathbf{u}^{*} \vartheta^{*} \cdot \nabla \phi \, \mathbf{d} \mathbf{x} \right) \psi(\mathbf{t}) \mathbf{d} \mathbf{t} \right| \\ & \leq \left| \int_{0}^{T} \left(\int_{\Omega} u_{m} \vartheta_{\mathbf{m}} \cdot \nabla \phi - \mathbf{u}_{\mathbf{m}} \vartheta^{*} \cdot \nabla \phi \, \mathbf{d} \mathbf{x} \right) \psi(\mathbf{t}) \mathbf{d} \mathbf{t} \right| \\ & + \left| \int_{0}^{T} \left(\int_{\Omega} u_{m} \vartheta^{*} \cdot \nabla \phi - \mathbf{u}^{*} \vartheta^{*} \cdot \nabla \phi \, \mathbf{d} \mathbf{x} \right) \psi(\mathbf{t}) \mathbf{d} \mathbf{t} \right| \end{split}$$



$$\leq \left| \int_{0}^{T} u_{m} \left(\int_{\Omega} (\vartheta_{\mathbf{m}} - \vartheta) \cdot \nabla \phi \, \mathbf{dx} \right) \psi(t) dt + \left| \int_{0}^{T} (u - u_{m}) \left(\int_{\Omega} \mathbf{v} \vartheta^{*} \cdot \nabla \phi \, dx \right) \psi(t) \, dt \right|$$

$$\leq \|u_{m}\|_{L^{\infty}(0,t_{f})} \|\|\mathbf{L}^{\infty}\| \vartheta_{\mathbf{m}} - \vartheta^{*}\|_{\mathbf{L}^{2}(\mathbf{0},\mathbf{t_{f}};\mathbf{L}^{2}(\Omega))} \|\nabla \phi\|_{\mathbf{L}^{2}} \|\psi\|_{\mathbf{L}^{2}(\mathbf{0},\mathbf{t_{f}})}$$

$$+ \left| \int_{0}^{T} (u^{*} - u_{m}) \left(\int_{\Omega} \mathbf{v} \vartheta^{*} \cdot \nabla \phi \, dx \right) \psi(t) \, dt \right| \to 0,$$

(2024) 89:57

where the last term converges to zero is because

$$\sup_{t\in[0,t_f]}\int_{\Omega}\mathbf{v}\vartheta^*\cdot\nabla\phi\,dx\leq\sup_{t\in[0,t_f]}\|\mathbf{v}\|_{L^\infty}\|\vartheta^*\|_{L^2}\|\nabla\phi\|_{L^2}\leq\|\mathbf{v}\|_{L^\infty}\|\vartheta^*\|_{L^\infty(0,t_f;L^2(\Omega))}\|\nabla\phi\|_{L^2},$$

thus $\int_{\Omega} \mathbf{v} \vartheta^* \cdot \nabla \phi \, dx \in L^{\infty}(0, t_f)$ and $(\int_{\Omega} \mathbf{v} \vartheta^* \cdot \nabla \phi \, dx) \psi(t) \in L^2(0, t_f)$. Due to the weak convergence of u_m in $L^2(0, t_f)$, the last terms converges to zero. Moreover,

$$\left| \int_{0}^{t_{f}} \left[(\vartheta_{m} \nabla c_{m}, \nabla \phi) - (\vartheta \nabla c, \nabla \phi) \right] \psi(t) dt \right| \\
= \left| \int_{0}^{t_{f}} \left(\int_{\Omega} \vartheta_{m} (\nabla c_{m} - \nabla c) \cdot \nabla \phi \, dx + \int_{\Omega} (\vartheta_{m} - \vartheta) \nabla c \cdot \nabla \phi \, dx \right) \psi(t) dt \right| \\
\leq \|\vartheta_{m}\|_{L^{2}(0,t_{f};H^{1}(\Omega))} \|\nabla c_{m} - \nabla c\|_{L^{2}(0,t_{f};H^{1}(\Omega))} \|\nabla \phi\|_{L^{2}} \|\psi\|_{L^{\infty}(0,t_{f})} \\
+ \left| \int_{0}^{t_{f}} \left(\int_{\Omega} (\vartheta_{m} - \vartheta) \nabla c \cdot \nabla \phi \, dx \right) \psi(t) dt \right| \to 0, \tag{2.23}$$

where for the last term we have $\nabla c \cdot \nabla \phi \psi(t) \in L^2(0, t_f; (H^1(\Omega))')$. In fact, for any $g \in L^2(0, t_f; H^1(\Omega)),$

$$\left| \int_{0}^{t_{f}} \int_{\Omega} \nabla c \cdot \nabla \phi \psi(t) g \, dx \, dt \right| \leq \int_{0}^{t_{f}} \| \nabla c \|_{H^{1}} \| \nabla \phi \|_{L^{2}} \| g \|_{H^{1}} | \psi(t) | \, dt$$

$$\leq \| \nabla c \|_{L^{2}(0,t_{f};H^{1}(\Omega))} \| \nabla \phi \|_{L^{2}} \| g \|_{L^{2}(0,t_{f};H^{1}(\Omega))} \| \psi \|_{L^{\infty}(0,t_{f})},$$

which follows

$$\begin{split} \|\nabla c \cdot \nabla \phi \psi\|_{L^{2}(0,t_{f};(H^{1}(\Omega))')} &\leq \|\nabla c\|_{L^{2}(0,t_{f};H^{1}(\Omega))} \|\nabla \phi\|_{L^{2}} \|\psi\|_{L^{\infty}(0,t_{f})} \\ &\leq C \|\vartheta\|_{L^{2}(0,t_{f};L^{2}(\Omega))} \|\nabla \phi\|_{L^{2}} \|\psi\|_{L^{\infty}(0,t_{f})}. \end{split}$$

By (2.18), the last term of (2.23) converges to zero. In addition, we have

$$(\vartheta_0, \phi \psi(0)) = (\vartheta_0^*, \phi \psi(0)), \quad \forall \phi \in H^1(\Omega),$$

which indicates $\vartheta_0^* = \vartheta_0$. Therefore, ϑ^* is the solution corresponding to u^* . Finally, using the weakly lower semicontinuity property of norms in J yields

$$J(u^*) \le \underline{\lim}_{m \to \infty} J(u_m) = \inf_{u \in U_{\mathrm{ad}}} J(u),$$

which indicates that u^* is an optimal solution to problem (P).



3 First-Order Optimality Conditions

Since (P) is non-convex, we will deal with local solutions. We now derive the first-order necessary optimality conditions for problem (P) by using a variational inequality (e.g. [31]), that is, if J is Gâteaux differentiable with respect to u and u is an optimal solution of problem (P), then

$$J'(u) \cdot (h - u) \ge 0, \quad h \in U_{ad}.$$
 (3.1)

To justify that J is indeed Gâteaux differentiable with respect to u, it suffices to show that ϑ is Gâteaux differentiable with respect to u.

Lemma 3.1 Let $z = \vartheta'(u) \cdot h$ for $h \in U_{ad}$ be the Gâteaux derivative of ϑ with respect to u in the direction of h. Then z satisfies $\int_{\Omega} z \, dx = 0$ and

$$\frac{\partial z}{\partial t} = \Delta z - u \mathbf{v} \cdot \nabla z - h \mathbf{v} \cdot \nabla \vartheta - \nabla \cdot (z \nabla c) - \nabla \cdot ((\vartheta + \bar{\theta}) \nabla \mathcal{A}^{-1} z), \tag{3.2}$$

$$\frac{\partial z}{\partial \mathbf{n}}|_{\Gamma} = 0,\tag{3.3}$$

with initial condition

$$z(x,0) = 0. (3.4)$$

Moreover, there exists a unique solution to (3.2)–(3.4) and for any $0 < t_f < \infty$,

$$z \in C([0, t_f]; H) \cap L^2(0, t_f; H^1(\Omega)).$$
 (3.5)

Proof Applying an L^2 -estimate together with Hölder's inequality and Ladyzhenskaya's inequality that $||f||_{L^4} \le C||f||_{L^2}^{1-d/4} ||\nabla f||_{L^2}^{d/4}, d=2,3$ (e.g. [7, p.55]), and the boundary conditions in (1.12) and (3.3) yields

$$\begin{split} \frac{1}{2} \frac{d \|z\|_{L^{2}}^{2}}{dt} + \|\nabla z\|_{L^{2}}^{2} &= -\frac{1}{2} u \int_{\Omega} \mathbf{v} \cdot \nabla z^{2} \, dx - \int_{\Omega} h \mathbf{v} \cdot \nabla \vartheta z \, dx - \int_{\Gamma} z \nabla c \cdot \mathbf{n} z \, dx \\ &+ \int_{\Omega} z \nabla c \cdot \nabla z \, dx \\ &- \int_{\Gamma} ((\vartheta + \bar{\theta}) \nabla \mathcal{A}^{-1} z) \cdot \mathbf{n} z \, dx + \int_{\Omega} (\vartheta + \bar{\theta}) \nabla \mathcal{A}^{-1} z \cdot \nabla z \, dx \\ &= h \int_{\Omega} \vartheta \mathbf{v} \cdot \nabla z \, dx + \int_{\Omega} z \nabla c \cdot \nabla z \, dx + \int_{\Omega} (\vartheta + \bar{\theta}) \nabla \mathcal{A}^{-1} z \cdot \nabla z \, dx \\ &\leq |h|_{L^{\infty}} \|\vartheta\|_{L^{2}} \|\mathbf{v}\|_{L^{\infty}} \|\nabla z\|_{L^{2}} + \|z\|_{L^{4}} \|\nabla c\|_{L^{4}} \|\nabla z\|_{L^{2}} \\ &+ \|\vartheta + \bar{\theta}\|_{L^{4}} \|\nabla \mathcal{A}^{-1} z\|_{L^{4}} \|\nabla z\|_{L^{2}} \\ &\leq C|h|_{L^{\infty}}^{2} \|\vartheta\|_{L^{2}}^{2} \|\mathbf{v}\|_{L^{\infty}}^{2} + \frac{1}{6} \|\nabla z\|_{L^{2}}^{2} + C\|z\|_{L^{2}}^{1-d/4} \|\nabla z\|_{L^{2}}^{d/4} \|\nabla \mathcal{A}^{-1} \vartheta\|_{H^{1}} \|\nabla z\|_{L^{2}} \end{split}$$

$$(3.6)$$



$$+ C \|\vartheta + \bar{\theta}\|_{H^{1}}^{2} \|\nabla \mathcal{A}^{-1}z\|_{H^{1}}^{2} + \frac{1}{6} \|\nabla z\|_{L^{2}}^{2}. \tag{3.7}$$

For the third term in (3.6) we use Young and Poincaré's inequalities and obtain

$$||z||_{L^{2}}^{1-d/4} ||\nabla z||_{L^{2}}^{d/4} ||\nabla \mathcal{A}^{-1}\vartheta||_{H^{1}} ||\nabla z||_{L^{2}} \leq C ||z||_{L^{2}}^{2} ||\nabla \mathcal{A}^{-1}\vartheta||_{H^{1}}^{\frac{8}{4-d}} + \frac{1}{6} ||\nabla z||_{L^{2}}^{2}$$

$$\leq C ||z||_{L^{2}}^{2} ||\vartheta||_{L^{2}}^{\frac{8}{4-d}} + \frac{1}{6} ||\nabla z||_{L^{2}}^{2}. \tag{3.8}$$

Combining (3.6)–(3.7) with (3.8) follows

$$\frac{d\|z\|_{L^{2}}^{2}}{dt} + \|\nabla z\|_{L^{2}}^{2} \leq C|h|_{L^{\infty}}^{2} \|\vartheta\|_{L^{2}}^{2} \|\mathbf{v}\|_{L^{\infty}}^{2} + C\|z\|_{L^{2}}^{2} \|\vartheta\|_{L^{2}}^{\frac{8}{4-d}} + C(\|\vartheta\|_{H^{1}}^{2} + |\bar{\theta}|^{2}) \|z\|_{L^{2}}^{2}, \tag{3.9}$$

and hence by Grönwall's inequality and (2.12) we obtain

$$\sup_{t \in [0, t_f]} \|z\|_{L^2}^2 \le C \|\mathbf{v}\|_{L^{\infty}}^2 \int_0^{t_f} |h|_{L^{\infty}}^2 \|\vartheta\|_{L^2}^2 dt \cdot e^{C \int_0^{t_f} (\|\vartheta\|_{L^2}^{\frac{8}{4-d}} + \|\vartheta\|_{H^1}^2 + |\bar{\theta}|^2) dt} < \infty.$$
(3.10)

Moreover, from (3.9)–(3.10) it follows

$$\int_0^{t_f} \|\nabla z\|_{L^2}^2 < \infty. \tag{3.11}$$

Finally, with the help of *a priori* estimates (3.10)–(3.11) and the Galerkin approximation, one can show that there exists a unique solution to (3.2)–(3.4). In other words, *z* is well-defined and this completes the proof.

Lemma 3.1 indicates that ϑ is Gâteaux differentiable with respect to $u \in U_{ad}$, so is J. A direct calculation follows that

$$J'(u) \cdot h = \alpha(\vartheta(t_f), z(t_f)) + \beta \int_0^{t_f} (\vartheta, z) \, dt + \gamma \int_0^{t_f} uh \, dt, \quad \forall h \in U_{ad}. \quad (3.12)$$

Theorem 3.2 Assume that $\vartheta_0 \in L^\infty(\Omega)$ and $\mathbf{v} \in L^\infty(\Omega)$. If u(t) is an optimal solution to problem (P) and ϑ is the corresponding solution to the state equations. Then there exists an adjoint state ρ such that the optimal triplet (u, ϑ, ρ) satisfies

State Equations $\begin{cases} \frac{\partial \vartheta}{\partial t} = \Delta \vartheta - u \mathbf{v} \cdot \nabla \vartheta - \nabla \cdot ((\vartheta + \bar{\vartheta}) \nabla c), \\ -\Delta c + c = \vartheta + \bar{\theta}, \\ \frac{\partial \theta}{\partial \mathbf{n}} \Big|_{\Gamma} = \frac{\partial c}{\partial \mathbf{n}} \Big|_{\Gamma} = 0, \\ \theta(0) = \theta_{0}, \end{cases}$ (3.13)



Adjoint Equations
$$\begin{cases} -\frac{\partial \rho}{\partial t} = \Delta \rho + u\mathbf{v} \cdot \nabla \rho + \nabla c \cdot \nabla \rho - \mathcal{A}^{-1}(\nabla \cdot (\vartheta \nabla \rho)) + \beta \vartheta, \\ \frac{\partial \rho}{\partial \mathbf{n}}\Big|_{\Gamma} = 0, \\ \rho(t_f) = \alpha \vartheta(t_f), \end{cases}$$

(3.14)

Optimality condition:
$$u^{opt}(t) = \mathbb{P}_{[\underline{u},\overline{u}]} \left(-\frac{1}{\gamma} \int_{\Omega} (\vartheta \nabla \rho) \cdot \mathbf{v} \, dx \right),$$
 (3.15)

where for real numbers $c \leq d$, $\mathbb{P}_{[c,d]}$ denotes the projection of \mathbb{R} onto [c,d], that is, $\mathbb{P}_{[c,d]}(f) := \min\{d, \max\{c, f\}\}.$

Proof To define the adjoint state, we take the inner product of (3.2) with ρ

$$\int_{0}^{t_{f}} \left(\frac{\partial z}{\partial t}, \rho\right) dt = \int_{0}^{t_{f}} (\Delta z, \rho) dt - \int_{0}^{t_{f}} u(\mathbf{v} \cdot \nabla z, \rho) dt - \int_{0}^{t_{f}} (h\mathbf{v} \cdot \nabla \theta, \rho) dt - \int_{0}^{t_{f}} (\nabla \cdot (z\nabla c), \rho) dt - \int_{0}^{t_{f}} (\nabla \cdot ((\vartheta + \bar{\theta})\nabla A^{-1}z), \rho) dt,$$
(3.16)

which follows

$$(\rho(t_f), z(t_f)) - (\rho(0), z(0)) + \int_0^{t_f} (-\frac{\partial \rho}{\partial t}, z) dt$$

$$= \int_0^{t_f} (\Delta \rho, z) dt + \int_0^{t_f} u(\mathbf{v} \cdot \nabla \rho, z) dt + \int_0^{t_f} (\theta \nabla \rho, \mathbf{v}) dt dt$$

$$+ \int_0^{t_f} (z \nabla c, \nabla \rho) dt - \int_0^{t_f} (z, \mathcal{A}^{-1}(\nabla \cdot ((\vartheta + \bar{\theta}) \nabla \rho))) dt.$$
(3.17)

Let ρ satisfy

$$-\frac{\partial \rho}{\partial t} = \Delta \rho + \mathbf{v} \cdot \nabla \rho + \nabla c \cdot \nabla \rho - \mathcal{A}^{-1}(\nabla \cdot ((\vartheta + \bar{\theta})\nabla \rho)) + \beta \vartheta, \tag{3.18}$$

$$\frac{\partial \rho}{\partial \mathbf{n}}|_{\Gamma} = 0, \tag{3.19}$$

with final time condition

$$\rho(t_f) = \alpha \vartheta(t_f). \tag{3.20}$$

Then combining (3.17) with (3.18)–(3.20) follows

$$(\alpha \vartheta(t_f), z(t_f)) = \int_0^{t_f} (\theta \nabla \rho, \mathbf{v}) h \, dt - \int_0^{t_f} (\beta \vartheta, z) \, dt.$$
 (3.21)



As a result, if u is an optimal solution, then by (3.12)

$$J'(u) \cdot h = \int_0^{t_f} (\theta \nabla \rho, \mathbf{v}) h \, dt + \gamma \int_0^{t_f} u h \, dt \ge 0, \tag{3.22}$$

for any $h \in U_{ad}$, which establishes (3.15).

3.1 Control of Cellular Flows in Rectangle-Like Domains

In real life applications, however, many flows are not necessarily relaxation-enhancing, i.e., (2.5) may not be satisfied. The semigroup generated by the advection–diffusion operator can still have the rapid decay property. As shown in (e.g. [17, 18]), for the velocity field generated by cellular flows in rectangle-like domains (rectangles (d=2) and parallelepipeds (d=3)), rescaling both the cell size and the flow amplitude is able to establish the rapid decay property of the semigroup generated by the associated advection–diffusion operator. It is important to point out that in rectangle-like domains our main theorems in this work still hold.

To demonstrate the idea, we consider the following prototypical example of a 2D cellular flow for our numerical tests

$$\mathbf{v}(x,y) = \nabla^{\perp} \sin(2\pi x) \sin(2\pi y) = 2\pi \begin{bmatrix} -\sin(2\pi x)\cos(2\pi y) \\ \cos(2\pi x)\sin(2\pi y) \end{bmatrix}$$
(3.23)

in a two-dimensional domain $\Omega=(0,1)^2$. For d=3, one can utilize the cubic cells given by (e.g. [3, 18, 38]). Since the cellular flows and the basis functions are periodic, they can be naturally extended to $N\Omega=(0,N)^d$ for $N\in\mathbb{N}^+$.

Let $\mathcal{L}_1 = \Delta - \mathbf{v}(x) \cdot \nabla$, where $x = (x_1, \dots, x_d)$ and $\mathbf{v} = (v_1, \dots, v_d)$, d = 2, 3, with $D(\mathcal{L}_1) = \{ \psi \in H^2(\Omega) \cap H : \frac{\partial \psi}{\partial \mathbf{n}} |_{\Gamma} = 0 \}$. Let $v_{i_N}(x) = v_i(Nx)$ for $x \in \Omega$, $N \in \mathbb{N}^+$, and $\mathbf{v}_N = (v_{1_N}, \dots, v_{d_N})$, d = 2, 3. According to (3.23), the rescaled cellular flow velocity \mathbf{v}_N is still sufficiently smooth and periodic, yet with higher frequency compared to \mathbf{v} . Now define

$$\mathcal{L}_N = \Delta - N\mathbf{v}_N(x) \cdot \nabla$$

with $D(\mathcal{L}_N) = D(\mathcal{L}_1)$. One can show that

$$\Psi_N = N^2 \Psi_1, \tag{3.24}$$

where $\Psi_N = \Psi(\mathcal{L}_N)$ is defined as in (2.2) for $N \in \mathbb{N}^+$. The detailed proof is given by [17, Proposition 3.1]. Therefore,

$$||e^{\mathcal{L}_N t}||_{\mathcal{L}(H)} \le M_0 e^{-\Psi_N t} = M_0 e^{-N^2 \Psi_1 t}, \quad t \ge 0,$$

which indicates that the decay rate of the semigroup $e^{\mathcal{L}_N t}$ can be made arbitrarily fast if N is sufficiently large. According to Theorem 2.2, for a given initial condition ϑ_0 , as



long as the amplitude and the ordinary frequency $N = N(\vartheta_0, \bar{\theta})$ of the cellular flows are large enough, the system is well-posed and exponentially stable.

For a fixed flow frequency, the objective of the optimal control design using cellular flows is to determine an optimal time-dependent flow amplitude u(t) to regulate the strength of the flow. The existence of such a solution follows from Theorem 2.4. It is clear that it suffices to choose the upper bound of u(t) satisfying $\overline{u} \ge N(\vartheta_0, \overline{\theta})$. Again we can simply set $\underline{u} = -\overline{u}$. Numerical experiments based on cellular flows will be presented in the next section to demonstrate our control design.

4 Numerical Implementation

In this section, we present our numerical experiments for the suppression of singularity of the PKS system in rectangle domains by utilizing the 2D cellular flows introduced in Sect. 3.1. We use the spline collocation method to solve the optimality system (3.13)–(3.15) along with the Euler forward method in time. The bivariate spline functions are employed to approximate the system based on the weak formulation for parabolic-elliptic PDEs. For the convenience of the reader, we provide a brief explanation in Appendix 1. One can refer to [1, 10, 25–27] for a detailed study.

To validate the accuracy of our algorithms for solving the PKS system without flow advection, we present numerical tests in Appendix A.1. In particular, we verify the validity of the algorithm for conservation of mass and non-negativity of the solutions θ and c. Following the main results in Theorem 3.2, we implement the optimality system (3.13)–(3.15) using Algorithm 4.1 presented below. For computational convenience, we replace ϑ by $\theta - \bar{\theta}$.

Algorithm 4.1: Adjoint Method for Optimal Control Problems

Given a final time $t_f > 0$, a tolerance $\epsilon > 0$, and constants $\alpha, \beta, \gamma > 0$, for j = 1, 2, ..., we compute u^j using the following iterations with known u^{j-1} :

• **Step 1**: First, we use the initial function $u^{j-1}(t)$ and the given $\mathbf{v}(x, y)$. Let $\theta(0, x) = \theta_0(x) \ge 0$ and $c_0(x) = c(0, x)$. Solve

$$-\Delta c_0(x) + c_0(x) = \theta_0$$
 and $\frac{\partial c_0}{\partial \mathbf{n}}\Big|_{\Gamma} = 0$.

Let $u_k = u^{j-1}(t_k)$. Solve $\theta_k = \theta(t_k, x)$ and $c_k = c(t_k, x)$ at each time step $t_k, k = 1, 2, \dots, n$, where $n = [\frac{t_f}{\Delta t}]$, from the following equations

$$\frac{\theta_k - \theta_{k-1}}{\Delta t} = \kappa \, \Delta \theta_{k-1} - u_k \mathbf{v} \cdot \nabla \theta_{k-1} - \nabla \cdot (\theta_{k-1} \nabla c_{k-1}), \quad \frac{\partial \theta_k}{\partial \mathbf{n}} \big|_{\Gamma} = 0,$$

and

$$-\Delta c_k(x) + c_k(x) = \theta_k$$
 and $\frac{\partial c_k}{\partial \mathbf{n}}|_{\Gamma} = 0$.

Stop if $|\theta|_{\infty} > 5$, 000 and set $t_f = t_n$.



• Step 2 : Compute $\rho_n = \alpha(\theta_n - \bar{\theta}_n)$ using $t_f = t_n$ and $w_n = \mathcal{A}^{-1}(\nabla \cdot (\theta_n \nabla \rho_n))$, that is, we solve

(2024) 89:57

$$(-\Delta + I)w_n = \nabla \cdot (\theta_n \nabla \rho_n)$$
 and $\frac{\partial w_n}{\partial \mathbf{n}}|_{\Gamma} = 0$.

• Step 3: Set $t_f = t_n$. Use ρ_n , θ_n and c_n to solve ρ_{n-1} backward in time from the adjoint equations

$$-\frac{\rho_n - \rho_{n-1}}{\Delta t} = \kappa \Delta \rho_n + u_n \mathbf{v} \cdot \nabla \rho_n + \nabla c_n \cdot \nabla \rho_n - w_n + \beta (\theta_n - \bar{\theta}_n),$$

$$\frac{\partial \rho_{n-1}}{\partial \mathbf{n}} \Big|_{\Gamma} = 0.$$

• Step 4: For given ρ_{n-1} and θ_{n-1} , compute w_{n-1} from

$$(-\Delta + I)w_{n-1} = \nabla \cdot (\theta_{n-1} \nabla \rho_{n-1}).$$

• **Step 5**: Find ρ_{n-2} that satisfies

$$\rho_{n-2} = \rho_{n-1} + \Delta t (\kappa \Delta \rho_{n-1} + u_{n-1} \mathbf{v} \cdot \nabla \rho_{n-1} + \nabla c_{n-1} \cdot \nabla \rho_{n-1} - w_{n-1} + \beta (\theta_{n-1} - \bar{\theta}_{n-1})),$$

$$\frac{\partial \rho_{n-2}}{\partial \mathbf{n}} \Big|_{\Gamma} = 0.$$

Repeat **Steps 4–5** to solve $\rho_{n-3}, \dots, \rho_0$.

• Step 6 : Compute

$$u_j(t_k) = \mathbb{P}_{[\underline{u},\overline{u}]} \left(-\frac{1}{\gamma} \int_{\Omega} (\theta_k \nabla \rho_k) \cdot \mathbf{v} \, dx \right), \quad k = 0, 1, \dots, n.$$

where $\mathbb{P}_{[u,\overline{u}]}$ denotes the projection of \mathbb{R} onto $[\underline{u},\overline{u}]$, that is, $\mathbb{P}_{[u,\overline{u}]}(f)$ $:= \min\{\overline{u}, \max\{\underline{u}, f\}\}$

• Stop, if $\frac{|J(u^j) - J(u^{j-1})|}{I(u^{j-1})} < \epsilon.$

We begin with demonstrating the development of singularity in the solution to the PKS system in finite time when there is no flow advection and the initial condition is above a certain threshold. We then present our optimal control design for suppressing such singularity formation. Nagai in [32] considered the system (1.1)–(1.5) without advection in a 2D disk and showed that under the condition $\theta_0 > 8\pi$, the radial solution blows up in finite time if $\int_{\Omega} \theta_0 |x|^2 dx$ is sufficiently small. However, under the condition $\bar{\theta}_0 < 8\pi$, the radial solution exists globally in time. In our numerical simulations, we first consider different Gaussian functions as the initial data as in [5] to demonstrate the density evolution, in response to the influence of a chemoattractant governed by the PKS system (1.1)–(1.5) without flow advection.



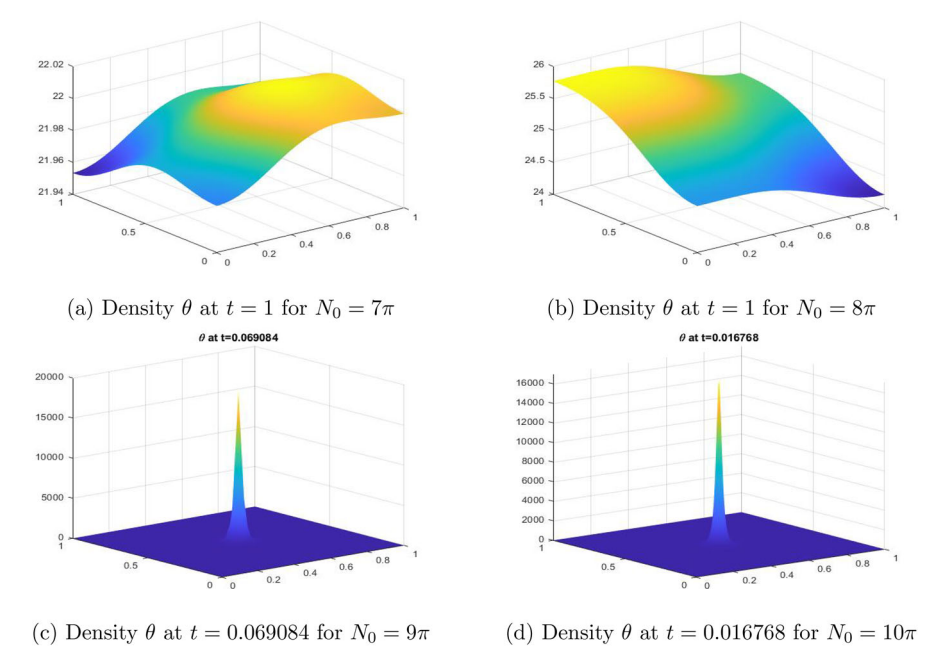


Fig. 1 Density θ with $(x_0, y_0) = (0.5, 0.5)$ for various initial mass

Example 4.1 Let $\Omega = (0, 1) \times (0, 1)$ and consider the following Gaussian function:

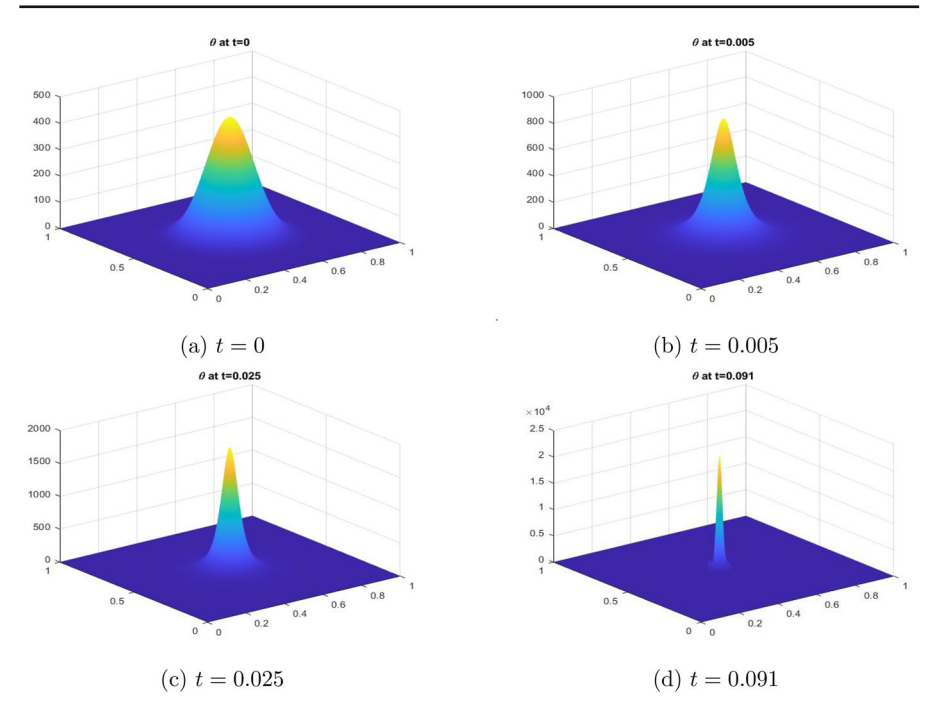
$$\theta_0 = \frac{N_0}{2\pi\rho} \exp\left(-\frac{(x-x_0)^2 + (y-y_0)^2}{2\rho}\right), \quad N_0 \in \mathbb{N}^+, \quad \rho > 0,$$

where $(x_0, y_0) = (0.5, 0.5)$. It is easy to check that $N_0(1 - e^{-\frac{1}{8\rho}}) < \int_{\Omega} \theta_0 dx < N_0(1 - e^{-\frac{1}{4\rho}})$. Thus $\int_{\Omega} \theta_0 dx \approx N_0$ if ρ is small. Set $\rho = 10^{-2}$ and the final time $t_f = 1$. We test different initial mass by letting N_0 be 7π , 8π , 9π , and 10π , respectively.

We set the mesh size $h=\frac{1}{8}$ and the time step $\Delta t=1e$ -5. Without flow advection, our results show that for $N_0 \leq 8\pi$ the density distribution approaches to its spatial average over time as shown in Figs. 1a–1b. However, for $N_0 > 8\pi$, the bump in the density function develops rapidly during evolution as shown in Figs. 1c–1d. For the latter, we refined the mesh near the center to get more accurate results. Figures 2a–2d demonstrate the density θ at various time steps for an initial mass about 9π with $(x_0, y_0) = (0.5, 0.5)$. We observe the rapid accumulation of mass toward the center, which indicates a possible singularity formation in finite time.

With the same settings as in Example 4.1, we now exemplify the PKS system with controlled flow advection and apply Algorithm 4.1 to solve the optimal system (3.13)–(3.15) for an optimal control.





(2024) 89:57

Fig. 2 Uncontrolled evolution of density θ with $(x_0, y_0) = (0.5, 0.5)$ and $N_0 = 9\pi$ at various time steps t = 0, 0.005, 0.025, 0.091

Example 4.2 Consider the same domain and initial data with $N_0 = 9\pi$ as in Example 4.1. We further consider the cellular flow given by

$$\mathbf{v}_{N}(x,y) = 2\pi \begin{pmatrix} -\sin(2N\pi x)\cos(2N\pi y) \\ \cos(2N\pi x)\sin(2N\pi y), \end{pmatrix}, \quad N \in \mathbb{N}^{+}, \tag{4.1}$$

as plotted in Fig. 3 for N = 1, 2. When u(t) = N is a constant, the density distribution θ blows up for N=1 but approaches to its spatial average for $N\geq 2$. Here we set $N=2, t_f=0.4, \alpha=\beta=1, \gamma=1, \overline{u}=N$ and $\underline{u}=-N$. The stop criterion in Algorithm 4.1 is set to be $\epsilon = 1e$ -08.

Figs. 4a-4d demonstrate the density evolution with optimally controlled flow advection for N=2 at t=0,0.005,0.01,0.4, respectively. The maximum value of θ in space decreases from 450 to 9π and the sharp peak is quickly suppressed by flow advection. Moreover, θ approaches to 9π as time evolves. The behavior of the optimal control input u(t) is presented in Fig. 5a, which first oscillates and switches between positive and negative values, and then converges to zero. This suggests that adjusting flow orientation is important in optimal control of flow advection, which may be more effective than simply increasing the flow strength for preventing the accumulation of mass according to our cost criteria. Figure 5b shows that the cost functional J(u)decreases and converges. In Fig. 5c, we observe that $\|\theta(t)\|_{L^{\infty}}$ quickly reaches the



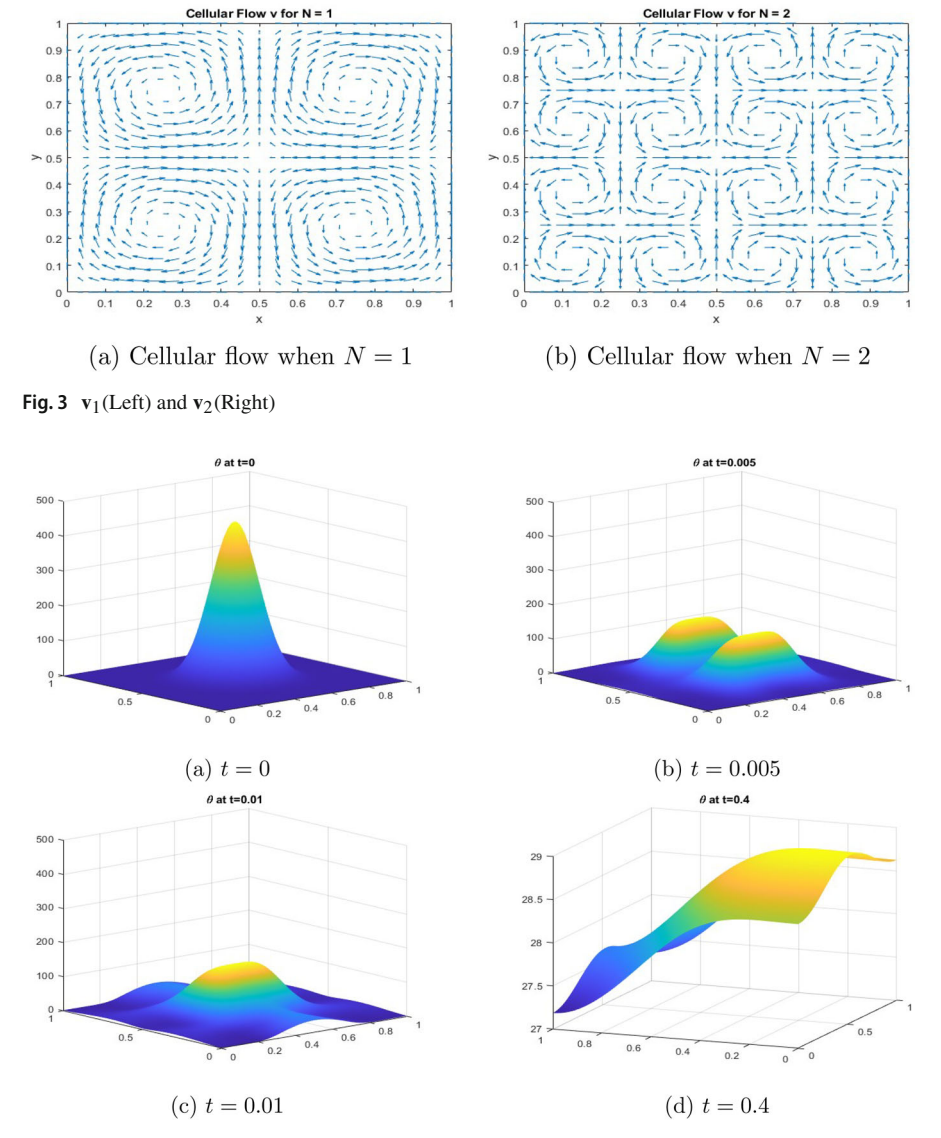


Fig. 4 Controlled evolution of density θ with $(x_0, y_0) = (0.5, 0.5)$, $N_0 = 9\pi$, N = 2, $\overline{u} = 2$ and $\underline{u} = -2$ at various time steps t = 0, 0.005, 0.01, 0.4

exponential decay rate for $t \in [0, 0.4]$ and converges to approximately 9π , which is close to the spatial average $\bar{\theta}$.

Next we investigate the effectiveness of flow advection with Gaussian initial data centered at different locations. We repeat the experiments for the Gaussian initial data with $N_0 = 9\pi$ and different centers (x_0, y_0) , where x_0 and y_0 take on the values of 0.4, 0.5, 0.6, 0.7. Initially, we set N = 2 in (4.1) and $\overline{u} = N$, but observe that θ blows up in all cases except for $(x_0, y_0) = (0.5, 0.5)$. To address this issue, we increase \overline{u} to



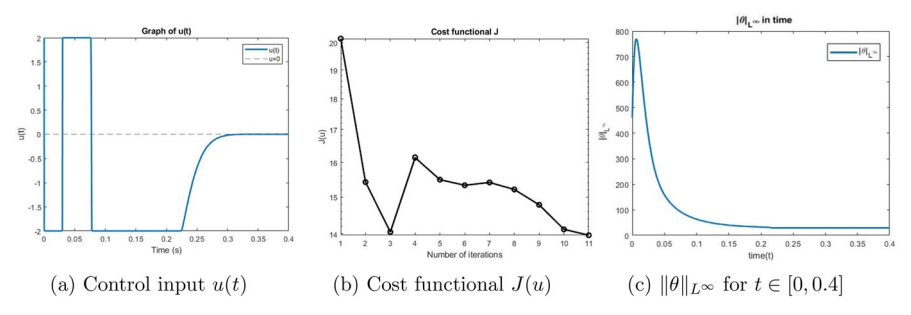


Fig. 5 Control input u(t), cost functional $J(u_j)$, $j=1,\cdots,11$, and $\|\theta(t)\|_{L^{\infty}}$ for $(x_0,y_0)=(0.5,0.5)$, N=2, $\overline{u}=2$, u=-2, and $t\in[0,0.4]$

20N and then θ does not blow up in any of these cases. As time progresses, we observe that the maximum value of θ decreases and θ approaches to its spatial average $\bar{\theta}$, which is about 9π for different centers $(x_0, y_0) = (0.4, 0.4), (0.4, 0.5), (0.4, 0.6)$, etc.

Example 4.3 We further examine the evolution of density θ by setting different upper bounds for the control input for a Gaussian initial datum centered at (0.7, 0.7) with $N_0 = 9\pi$.

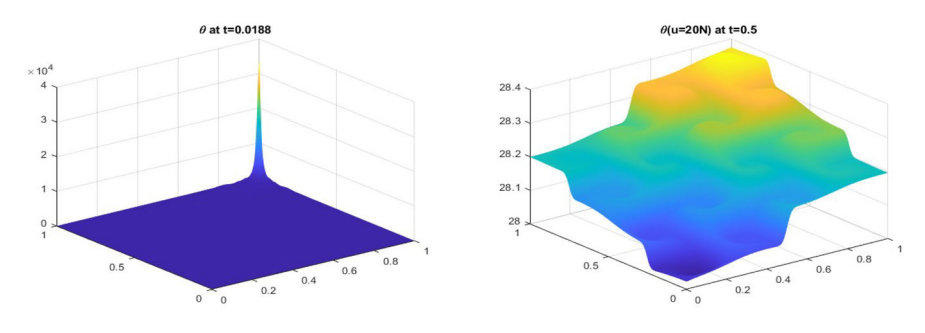
We take N=2 and first conduct forward simulations by letting $u(t)=\overline{u}$. Figures 6a-6b present the density distribution at t=0.0188 and t=0.5 for $u(t)=\overline{u}=N$ and $u(t)=\overline{u}=20N$, respectively. Figure 6a shows that the singularity formation occurs at the domain boundary for $u(t)=\overline{u}=2$ when t=0.0188. In contrast, as shown in Fig. 6b, increasing the upper bound \overline{u} to 40 results in a significantly faster decrease in the maximum value of θ and leads to convergence to its spatial average.

Now we set $\overline{u}=40$ and $\underline{u}=-40$ and apply Algorithm 4.1 for solving the optimal control. The optimal evolution of density is demonstrated in Figs. 7a–7d at t=0,0.003,0.01,0.4. The maximum value of θ decreases and θ approaches to its spatial average, which is about 9π . The behavior of the optimal control input u(t) is depicted in Fig. 8a. Similar to Example 4.2, it first oscillates and alternates between positive and negative values, and then converges to zero. Figure 8b illustrates the decrease and convergence of the cost functional J(u). Figure 8c shows that $\|\theta(t)\|_{L^\infty}$ quickly reaches the exponential decay rate for $t\in[0,0.4]$ and converges to approximately 9π . It is clear that both the flow magnitude and orientation affect the effectiveness of flow advection.

5 Conclusion

The idea of suppressing singularity formation via optimal control of flow advection is employed in this work for chemotaxis modeled by the PKS system, which leads to a nonlinear control and non-convex optimization problem. We established a rigorous proof of the existence of an optimal control and derived the first-order optimality conditions for solving such a control. Moreover, using spline collocation methods we conducted numerical experiments based on 2D cellular flows to validate the effec-





(a) Density θ at t = 0.0188 when $\overline{u} = N$

(b) Density θ at t = 0.5 when $\overline{u} = 20N$

Fig. 6 Density θ with $(x_0, y_0) = (0.7, 0.7)$ and different \overline{u} at t = 0.0188 and t = 0.5

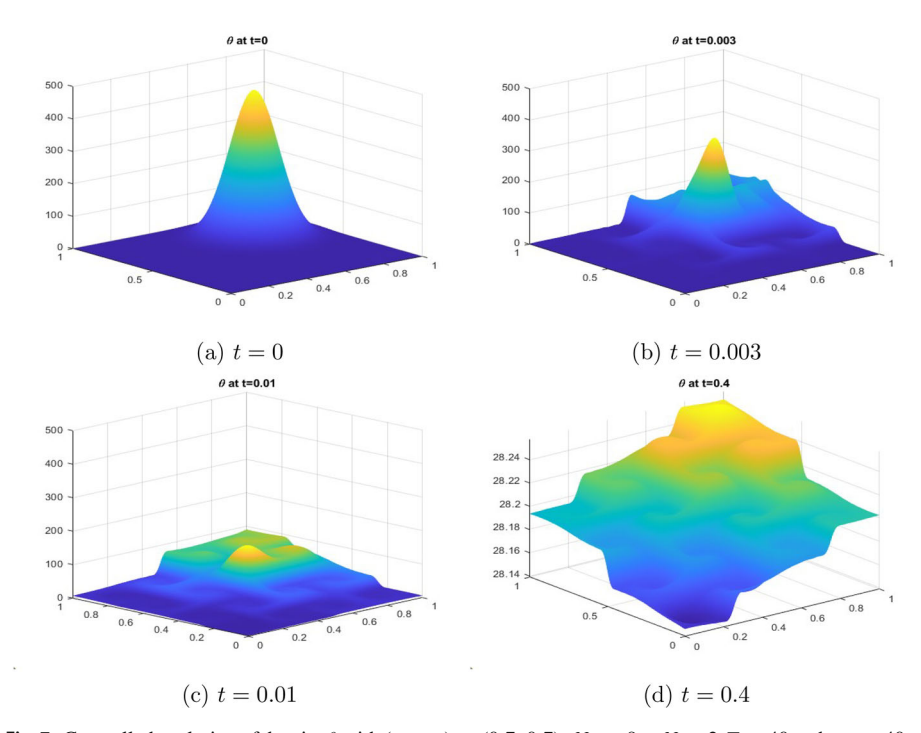


Fig. 7 Controlled evolution of density θ with $(x_0, y_0) = (0.7, 0.7)$, $N_0 = 9\pi$, N = 2, $\overline{u} = 40$ and $\underline{u} = -40$ at various time steps: t = 0, 0.003, 0.01, 0.4

tiveness of our control design. For the Gaussian type of initial data, we observed that treating different centers of the data may require different strength of the cellular flows in order to effectively suppress the singularity formation. On the other hand, varying the centers of cellular flows may help improve the efficiency for advection. This naturally gives rise to the question of what are the optimal locations for the cellular flow centers with respect to different initial data. We can further consider the linear combinations of the flows centered at different locations and with different magnitude for



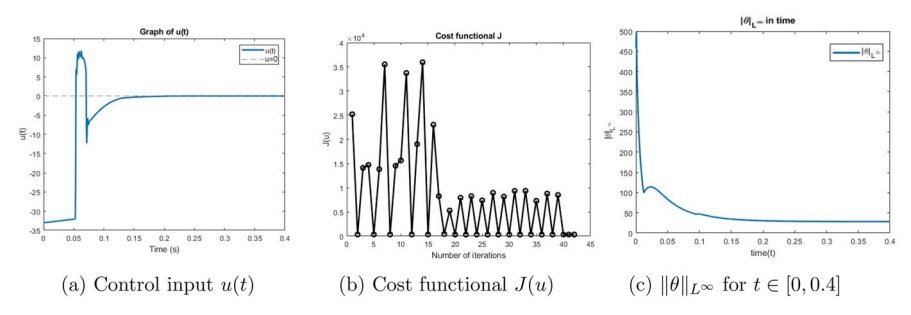


Fig. 8 Control input u(t), cost functional $J(u_j)$, $j=1,\cdots,42$, and $\|\theta(t)\|_{L^{\infty}}$ for $(x_0,y_0)=(0.7,0.7)$, N=2, $\overline{u}=40$, u=-40, and $t\in[0,0.4]$

generating the optimal velocity field. These topics will be further discussed in our future work.

Acknowledgements W. Hu was partially supported by the NSF Grants DMS-2005696 (previously DMS-1813570), DMS-2111486 and DMS-2205117. M.-J. Lai was partially supported by the Simons Foundation collaboration Grant No. 864439.

Declarations

Conflict of interest The authors have no relevant financial or non-financial interests to disclose.

Appendix

Bivariate Splines

Given a triangle T, we let |T| be the length of its longest edge, and ρ_T be the radius of the the largest disk that can be inscribed in T. For any polygonal domain $\Omega \subset \mathbb{R}^d$ with d=2, let $\Delta:=\{T_1,\cdots,T_n\}$ be a triangulation of Ω which is a collection of triangles and \mathcal{V} be the set of vertices of Δ . We called a triangulation as a quasi-uniform triangulation if all triangles T in Δ have comparable sizes in the sense that

$$\frac{|T|}{\rho_T} \le C < \infty$$
, all triangles $T \in \Delta$,

where ρ_T is the inradius of T. Let h be the length of the longest edge in Δ . For a triangle $T = (v_1, v_2, v_3) \in \Omega$, we define the barycentric coordinates (b_1, b_2, b_3) of a point $(x, y) \in \Omega$. These coordinates are the solution to the following system of equations

$$b_1 + b_2 + b_3 = 1,$$

 $b_1v_{1,x} + b_2v_{2,x} + b_3v_{3,x} = x,$
 $b_1v_{1,y} + b_2v_{2,y} + b_3v_{3,y} = y,$



where the vertices $v_i = (v_{i,x}, v_{i,y})$ for i = 1, 2, 3 and are nonnegative if $(x, y) \in T$. We use the barycentric coordinates to define the Bernstein polynomials of degree D:

$$B_{i,j,k}^{T}(x,y) := \frac{D!}{i!j!k!} b_1^i b_2^j b_3^k, \ i+j+k = D, \tag{A.1}$$

which form a basis for the space \mathcal{P}_D of polynomials of degree D. Therefore, we can represent all $s \in \mathcal{P}_D$ in B-form:

$$s|_T = \sum_{i+j+k=D} c_{ijk} B_{ijk}^T, \quad \forall T \in \Delta,$$

where the B-coefficients $c_{i,j,k}$ are uniquely determined by s.

Moreover, for given $T = (v_1, v_2, v_3) \in \Delta$, we define the associated set of domain points to be

$$\mathcal{D}_{D,T} := \left\{ \frac{iv_1 + jv_2 + kv_3}{D} \right\}_{i+j+k=D}.$$
 (A.2)

Let $\mathcal{D}_{D,\Delta} = \bigcup_{T \in \Delta} \mathcal{D}_{D,T}$ be the domain points of triangulation Δ and degree D.

We use the discontinuous spline space $S_D^{-1}(\Delta) := \{s | T \in \mathcal{P}_D, T \in \Delta\}$ as a base. Then we add the smoothness conditions to define the space $S_D^r := C^r(\Omega) \cap S_D^{-1}(\Delta)$. The smoothness conditions are explained in [27, Theorems 2.28 and 15.31]. Let \mathbf{c} be the coefficient vector of $s \in S_D^{-1}(\Delta)$ and H be the matrix which consists of the smoothness conditions across each interior edge of Δ . It is known that $H\mathbf{c} = 0$ if and only if $s \in C^r(\Omega)$ (e.g. [27]).

Computations involving splines written in B-form can be performed easily according to [1, 28, 29]. In fact, these spline functions have numerically stable, closed-form formulas for differentiation, integration, and inner products. If $D \ge 3r + 2$, spline functions on quasi-uniform triangulations have optimal approximation power.

Lemma A.1 [27, Lai and Schumaker, 2007] Let $k \geq 3r + 2$ with $r \geq 1$. Suppose Δ is a quasi-uniform triangulation of Ω . Then for every $u \in W_q^{k+1}(\Omega)$, there exists a quasi-interpolatory spline $s_u \in S_k^r(\Delta)$ such that

$$||D_x^{\alpha}D_y^{\beta}(u-s_u)||_{q,\Omega} \le Ch^{k+1-\alpha-\beta}|u|_{k+1,q,\Omega},$$

for a positive constant C dependent on u, r, k and the smallest angle of Δ , and for all $0 \le \alpha + \beta \le k$ with

$$|u|_{k,q,\Omega} := \left(\sum_{a+b=k} \|D_x^a D_y^b u\|_{L^q(\Omega)}^q\right)^{\frac{1}{q}}.$$

In this section, we explain the spline collocation method for solving the following PKS system in the absence of flow advection but with a nonzero force term f



together with the Euler forward method. We shall use the bivariate spline functions to approximate the solution of the PDE (e.g. [1, 25–27]).

$$\frac{\partial \theta}{\partial t} = \Delta \theta - \nabla \cdot (\theta \nabla c) + f \quad \text{in} \quad \Omega, \tag{A.3}$$

$$-\Delta c + c = \theta \quad \text{in} \quad \Omega, \tag{A.4}$$

$$\frac{\partial \theta}{\partial \mathbf{n}} = \frac{\partial c}{\partial \mathbf{n}} = 0 \quad \text{on} \quad \Gamma. \tag{A.5}$$

Bivariate splines have been used to solve similar PDEs in [10] with satisfactory numerical performance. In this literature, the computational method was based on the standard weak formulation. In the current work, we adopt the spline collocation method developed in [25], which produces a more accurate numerical solution than the bivariate splines based on the weak formulation for elliptic equations. Also, the spline collocation method is easy to implement without using a quadrature formula.

A.1 A Spline-Based Collocation Method for the Keller Segel Equation without Flow Advection

Let $\Omega \subset \mathbb{R}^2$ be a polygonal domain. Given an integer N_T and the final time $t_f > 0$, we let $\Delta t := \frac{t_f}{N_T}$ be the constant time-step and $t_k := k\Delta t$, for $k = 0, \dots, N_T - 1$. We consider a partitioning of the time interval $[0, t_f] = \bigcup_{k=0}^{N_T - 1} [t_k, t_{k+1}]$ and approximate the continuous-time derivative of the density using a forward Euler method

$$\frac{\partial \theta}{\partial t} \approx \frac{\theta_k - \theta_{k-1}}{\Delta t}.$$

Our computational scheme for the equations (A.3)–(A.5) is as follows:

Step 1: Using a given $\theta(0, x) = \theta_0(x)$, we get $c_0(x) = c(0, x)$ using the following equations

$$-\Delta c_0(x) + c_0(x) = \theta_0, \quad c_0(x) \ge 0, \quad \text{and} \quad \frac{\partial c_0}{\partial \mathbf{n}}|_{\Gamma} = 0. \tag{A.6}$$

Step 2: Find $\theta_k = \theta(t_k, x)$ from

$$\frac{\theta_k - \theta_{k-1}}{\Delta t} = \kappa \, \Delta \theta_{k-1} - \nabla \cdot (\theta_{k-1} \nabla c_{k-1}) + f_{k-1} \text{ in } \Omega, \tag{A.7}$$

$$\theta_k \ge 0 \text{ in } \Omega,$$
 (A.8)

$$\frac{\partial \theta_k}{\partial \mathbf{n}} = 0 \text{ on } \Gamma, \tag{A.9}$$

where $f_{k-1}(x) = f(t_{k-1}, x)$.



Step 3: Calculate $c_k = c(t_k, x)$ such that

$$-\Delta c_k(x) + c_k(x) = \theta_k, \quad c_k(x) \ge 0, \quad \text{and} \quad \frac{\partial c_k}{\partial \mathbf{n}}|_{\Gamma} = 0.$$
 (A.10)

Let us focus on how to solve (A.6) and (A.10). We first choose a set of domain points $\{\xi_i\}_{i=1,\dots,N}$ (cf. A.2) as collocation points and then use the spline basis functions \mathcal{B}^t_{α} (cf. A.1). Using these functions, we find the spline solution $\theta_k = \sum_{t \in \Delta} \sum_{|\alpha|=D} a_{\alpha}^{t,k} \mathcal{B}_{\alpha}^t$ in spline space $S_D^r(\Delta)$, $c_k = \sum_{t \in \Delta} \sum_{|\alpha|=D} b_{\alpha}^{t,k} \mathcal{B}_{\alpha}^t$ in the same spline space $S_D^r(\Delta)$ with the coefficient vectors $\mathbf{a}^k \ge 0$, $\mathbf{b}^k \ge 0$, respectively, satisfying

$$-\Delta c_k(\xi_i) + c_k(\xi_i) = \theta_k(\xi_i)$$
 and $\frac{\partial c_k(\xi_i)}{\partial \mathbf{n}}|_{\Gamma} = 0, k = 0, 1, \dots N_T,$

where $\{\xi_i\}_{i=1,\dots,N} \in \mathcal{D}_{D,\Delta}$ are the domain points of Δ of degree D. We can rewrite the above equation as the matrix equation:

$$(-K + MV)\mathbf{b}^k = MV\mathbf{a}^k$$
 and $B\mathbf{b}^k = 0$,

where $K = MxxV + MyyV = \left[\partial_{xx}\mathcal{B}_{\alpha}^{t}(x_{i}, y_{i})\right] + \left[\partial_{yy}\mathcal{B}_{\alpha}^{t}(x_{i}, y_{i})\right], MV =$ $[\mathcal{B}_{\alpha}^{t}(x_{i}, y_{i})]$ and $B\mathbf{b}^{k} = 0$ is associated with the boundary condition. Also, we add the smoothness conditions in terms of smooth matrix equation: $H\mathbf{b}^k = 0$. Hence, our spline collocation method is to find \mathbf{b}^k by solving the following constrained minimization:

$$\min_{\mathbf{b}^k} J(\mathbf{b}^k) = \frac{1}{2} \| (-K + MV)\mathbf{b}^k - MV\mathbf{a}^k \|^2$$
 (A.11)

subject to
$$B\mathbf{b}^{k} = 0$$
, $H\mathbf{b}^{k} = 0$, $\mathbf{b}^{k} \ge 0$. (A.12)

It is easy to see that such a constrained minimization has a unique solution as the feasible set is convex and the minimizing functional is convex. We shall use the iterative method in [25] to solve the above constrained minimization problem.

Similarly, we can solve the PDE in Step 2, i.e., (A.7) by finding the spline approximation θ_k which satisfies the following collocation equations

imation
$$\theta_k$$
 which satisfies the following collocation equations
$$\begin{cases} \theta_k(\xi_i) = \theta_{k-1}(\xi_i) + \Delta t (\kappa \Delta \theta_{k-1}(\xi_i) - \nabla \cdot (\theta_{k-1}(\xi_i) \nabla c_{k-1}(\xi_i)) + f_{k-1}(t_{k-1}, \xi_i)), \\ \frac{\partial \theta_k(\xi_i)}{\partial \mathbf{n}}|_{\Gamma} = 0, \\ \bar{\theta}_k = \bar{\theta}_0, \end{cases}$$
(A.13)

where $\{\xi_i\}_{i=1,\dots,N} \in \mathcal{D}_{D,\triangle}$ are the domain points of \triangle of degree D. That is, we can find θ_k by solving the following constrained minimization problem:

$$\min_{\mathbf{a}^k} J(\mathbf{a}^k) = \frac{1}{2} \|MV\mathbf{a}^k - \mathbf{f}_u\|^2$$
 (A.14)

subject to
$$B\mathbf{a}^{k} = 0$$
, $H\mathbf{a}^{k} = 0$, $I\mathbf{a}^{k} = \bar{\theta}_{0}$, $\mathbf{a}^{k} \ge 0$, (A.15)



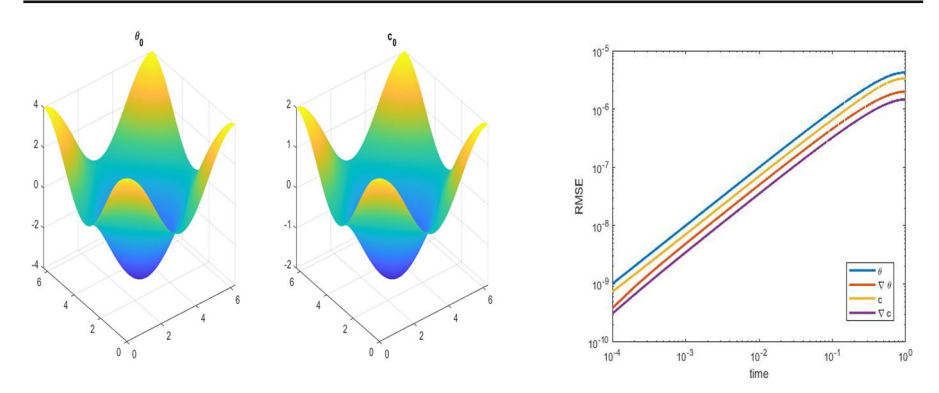


Fig. 9 Initial condition θ_0 (Left), numerical solution c_0 from Step 1 (Middle), and RMSEs for (θ, c) in Example A.2

where $I = [\int_{\Omega} \mathcal{B}_{\alpha}^{t}]$ is a row vector, B and 0 are derived from the boundary condition, \mathbf{f}_{u} is from the right side of the equation (A.13) and H is the matrix of all the smoothness conditions across each interior edge of triangulation Δ . Again, the above constrained minimization problem has a unique solution and we can use the iterative method in [25] to solve it. Repeating this process for each k, we can find the numerical solution to (A.3)–(A.5).

A.2 Numerical Examples for the PKS System Without Flow Advection

In this section, we present numerical experiments using the spline collocation method for solving PKS and demonstrate the accuracy of our algorithms. More simulation results can be found in [30].

We compute the root mean squared errors (RMSEs) of the approximate spline solution θ_s and c_s against the exact solutions θ and c based on 201 × 201 equally-spaced points over the bounding box of the domain Ω . The errors we compute include $\theta - \theta_s$, $\nabla(\theta - \theta_s)$, $c - c_s$, and $\nabla(c - c_s)$.

Example A.2 Let $\Omega = (-\pi, \pi)^2$. We consider the following exact solution satisfying (A.3)–(A.5)

$$\begin{cases} \theta = 2e^{-t}(\cos(x) + \cos(y)) \\ c = e^{-t}(\cos(x) + \cos(y)) \end{cases}$$

with an appropriate f. We choose the final time $t_f = 1$, $\Delta t = 1e$ -05, D = 10, r = 2, and a mesh size of $h = \pi/8$. Figure 9 shows the numerical solution of (θ, c) at t = 0 and the RMSEs of $\theta - \theta_s$, $\nabla(\theta - \theta_s)$, $c - c_s$, and $\nabla(c - c_s)$. The numerical errors are close to 1e-09 at the beginning and remain between 1e-05 and 1e-09.



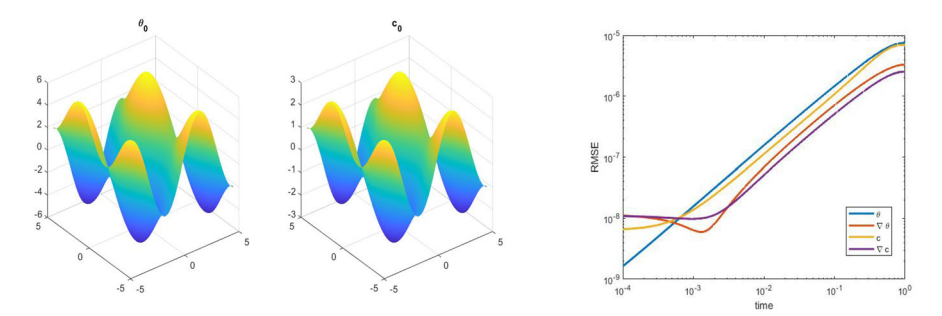


Fig. 10 Initial condition θ_0 (Left), numerical solution c_0 from Step 1 (Middle), and RMSEs for solution θ and c in Example A.3

Example A.3 Let $\Omega = (-\frac{3\pi}{2}, \frac{3\pi}{2})^2$. Consider the exact solution for (A.3)–(A.5) given by

$$\begin{cases} \theta = 2e^{-t}(2\sin(x) + \sin(y)) \\ c = e^{-t}(2\sin(x) + \sin(y)) \end{cases}$$

for an appropriate f. We use the same parameter settings as in Example A.2. Figure 10 presents the numerical solution of (θ, c) at t = 0 and the RMSEs of $\theta - \theta_s$, $\nabla(\theta - \theta_s)$, $c - c_s$ and $\nabla(c - c_s)$. Similar to the results of Example A.2, the RMSEs are between 1e-05 and 1e-09.

References

- Awanou, G., Lai, M.-J., Wenston, P.: The multivariate spline method for scattered data fitting and numerical solutions of partial differential equations. In: Wavelets and Splines: Athens, pp. 24–74. Nashboro Press, Brentwood (2005)
- Bedrossian, J., He, S.: Suppression of blow-up in Patlak–Keller–Segel via shear flows. SIAM J. Math. Anal. 49(6), 4722–4766 (2017)
- 3. Bisshopp, F.E.: On two-dimensional cell patterns. J. Math. Anal. Appl. 1(3-4), 373-385 (1960)
- Constantin, P., Kiselev, A., Ryzhik, L., Zlatoš, A.: Diffusion and mixing in fluid flow. Ann. Math. 168, 643–674 (2008)
- Filbet, F.: A finite volume scheme for the Patlak–Keller–Segel chemotaxis model. Numer. Math. 104(4), 457–488 (2006)
- Fister, K.R., McCarthy, C.M.: Optimal control of a chemotaxis system. Q. Appl. Math. 61, 193–211 (2003)
- Galdi, G.: An Introduction to the Mathematical Theory of the Navier–Stokes Equations: Steady-State Problems. Springer, Berlin (2011)
- Guillén-González, F., Mallea-Zepeda, E., Rodríguez-Bellido, M.: Optimal bilinear control problem related to a chemo-repulsion system in 2D domains. ESAIM 26, 29 (2020)
- Guillen-Gonzalez, F., Mallea-Zepeda, E., Rodriguez-Bellido, M.A.: A regularity criterion for a 3D chemo-repulsion system and its application to a bilinear optimal control problem. SIAM J. Control Optim. 58(3), 1457–1490 (2020)
- Gutierrez, J.B., Lai, M.-J., Slavov, G.: Bivariate spline solution of time dependent nonlinear PDE for a population density over irregular domains. Math. Biosci. 270, 263–277 (2015)
- Herrero, M.A.: Asymptotic properties of reaction-diffusion systems modeling chemotaxis. Appl. Ind. Math. Venice 2(1998), 89–108 (2000)



- Herrero, M.A., Veláizquez, J.J.L.: A blow-up mechanism for a chemotaxis model. Ann. Del. Scuola Norm. Super. Pisa Classe Sci. 24(4), 633 (1997)
- Herrero, M.A., Medina, E., Velázquez, J.J.L.: Finite-time aggregation into a single point in a reactiondiffusion system. Nonlinearity 10(6), 1739–1754 (1997)
- Herrero, M.A., Medina, E., Velázquez, J.J.L.: Self-similar blow-up for a reaction-diffusion system. J. Comput. Appl. Math. 97(1–2), 99–119 (1998)
- Horstmann, D.: The Keller–Segel model in chemotaxis and its consequences I. Jahresber. Deutsch. Math.-Verein. 105, 103–165 (1970)
- Horstmann, D.: From 1970 until present: the Keller–Segel model in chemotaxis and its consequences II. Jahresber. Deutsch. Math.-Verein. 106, 51–69 (2004)
- 17. Hu, W.: Global regularity and stability analysis of the Patlak–Keller–Segel system with flow advection in a bounded domain: a semigroup approach. Nonlinear Anal. 234, 113319 (2023)
- Iyer, G., Xiaoqian, X., Zlatoš, A.: Convection-induced singularity suppression in the Keller–Segel and other non-linear PDES. Trans. Am. Math. Soc. 374(09), 6039–6058 (2021)
- Jäger, W., Luckhaus, S.: On explosions of solutions to a system of partial differential equations modelling chemotaxis. Trans. Am. Math. Soc. 329(2), 819–824 (1992)
- 20. Kato, T.: Perturbation Theory for Linear Operators, vol. 132. Springer, New York (1966)
- Keller, E.F., Segel, L.A.: Initiation of slime mold aggregation viewed as an instability. J. Theoret. Biol. 26(3), 399–415 (1970)
- 22. Keller, E.F., Segel, L.A.: Model for chemotaxis. J. Theoret. Biol. 30(2), 225–234 (1971)
- Kiselev, A., Xiaoqian, X.: Suppression of chemotactic explosion by mixing. Arch. Ration. Mech. Anal. 222(2), 1077–1112 (2016)
- Lai, M.-J.: On construction of bivariate and trivariate vertex splines on arbitrary mixed grid partitions.
 Texas A&M University (1989)
- 25. Lai, M.-J., Lee, J.: A multivariate spline based collocation method for numerical solution of partial differential equations. SIAM J. Numer. Anal. **60**(5), 2405–2434 (2022)
- Lai, M.-J., Lee, J.: Trivariate spline collocation methods for numerical solution to 3D Monge–Ampére equation. J. Sci. Comput. 95, 1 (2023)
- Lai, M.-J., Schumaker, L.L.: Spline Functions over Triangulations. Cambridge University Press, Cambridge (2007)
- Lai, M.-J., Wang, C.: A bivariate spline method for second order elliptic equations in non-divergence form. J. Sci. Comput. 75, 803–829 (2018)
- 29. Lai, M.-J., Wenston, P.: Bivariate splines for fluid flows. Comput. Fluids 33(8), 1047–1073 (2004)
- 30. Lee, J.: A multivariate spline method for numerical solution of partial differential equations. PhD Dissertation, pp. 1–170 (2023)
- Lions, J.-L.: Optimal Control of Systems Governed by Partial Differential Equations. Springer, New York (1971)
- 32. Nagai, T.: Blow-up of radially symmetric solutions to a chemotaxis system. Adv. Math. Sci. Appl. 5, 581–601 (1995)
- Patlak, C.S.: Random walk with persistence and external bias. Bull. Math. Biophys. 15(3), 311–338 (1953)
- 34. Perthame, B., Dalibard, A.-L.: Existence of solutions of the hyperbolic Keller–Segel model. Trans. Am. Math. Soc. **361**(5), 2319–2335 (2009)
- Rodríguez-Bellido, M., Rueda-Gómez, D.A., Villamizar-Roa, É.J.: On a distributed control problem for a coupled chemotaxis-fluid model. Discret. Contin. Dyn. Syst. B 23(2), 557 (2018)
- Ryu, S.-U.: Boundary control of chemotaxis reaction diffusion system. Honam Math. J. 30(3), 469–478 (2008)
- Ryu, S.U., Yagi, A.: Optimal control of Keller–Segel equations. J. Math. Anal. Appl. 256(1), 45–66 (2001)
- 38. Ryzhik, L., Zlatoš, A.: Kpp pulsating front speed-up by flows. Commun. Math. Sci. 5(3), 575–593 (2007)
- Senba, T., Suzuki, T.: Applied Analysis: Mathematical Methods in Natural Science. World Scientific, Singapore (2011)
- 40. Suzuki, T.: Free Energy and Self-Interacting Particles. Springer, Berlin (2005)
- 41. Wei, D.: Diffusion and mixing in fluid flow via the resolvent estimate. Science China Math. **64**(3), 507–518 (2021)



Publisher's Note Springer Nature remains neutral with regard to jurisdictional claims in published maps and institutional affiliations.

Springer Nature or its licensor (e.g. a society or other partner) holds exclusive rights to this article under a publishing agreement with the author(s) or other rightsholder(s); author self-archiving of the accepted manuscript version of this article is solely governed by the terms of such publishing agreement and applicable law

